

# The effect of longitudinal density gradient on electron plasma wake field acceleration

David Tsiklauri

*School of Physics and Astronomy, Queen Mary University of London, London, E1 4NS, United Kingdom*

Three dimensional, particle-in-cell, fully electromagnetic simulations of electron plasma wake field acceleration in the blow out regime are presented. Earlier results are extended by (i) studying the effect of longitudinal density gradient; (ii) avoiding use of co-moving simulation box; (iii) inclusion of ion motion; and (iv) studying fully electromagnetic plasma wake fields. It is established that injecting driving and trailing electron bunches into a positive density gradient of ten-fold increasing density over 10 cm long Lithium vapor plasma, results in spatially more compact and three times larger, compared to the uniform density case, electric fields ( $-6.4 \times 10^{10}$  V/m), leading to acceleration of the trailing bunch up to 24.4 GeV (starting from initial 20.4 GeV), with an energy transfer efficiencies from leading to trailing bunch of 75 percent. In the uniform density case  $-2.5 \times 10^{10}$  V/m wake is created leading to acceleration of the trailing bunch up to 22.4 GeV, with an energy transfer efficiencies of 65 percent. It is also established that injecting the electron bunches into a negative density gradient of ten-fold decreasing density over 10 cm long plasma, results in spatially more spread and two-and-half smaller electric fields ( $-1.0 \times 10^{10}$  V/m), leading to a weaker acceleration of the trailing bunch up to 21.4 GeV, with an energy transfer efficiencies of 45 percent. Inclusion of ion motions into consideration shows that in the plasma wake ion number density can increase over few times the background value. It is also shown that transverse electromagnetic fields in plasma wake are of the same order as the longitudinal (electrostatic) ones.

## I. INTRODUCTION

Conventional particle accelerators have an accelerating gradient of tens of MV/m. The limit is set by the radio frequency (RF) breakdown phenomenon, when large electric field in the accelerator cavities causes accelerator to be effectively short-circuited. It is known that when electric field exceeds a threshold value, the Kilpatrick limit, no matter how good the vacuum in the accelerator tube is, there will be a RF breakdown and nearly all of the RF power is absorbed [4]. Thus the beam receives little or no acceleration in the cavity. Novel accelerator concepts that have a promise to overcome the difficulties of conventional particle accelerators include plasma wake field acceleration (PWFA), amongst a number of other concepts such as fixed-field alternating-gradient accelerators, dielectric wall accelerators, and dielectric laser accelerators. Plasma wake field acceleration usually refers to an acceleration of particles through the generation of strong electric fields from charged particle motion in plasma. Generally a distinction is drawn between beam-driven PWFA and laser-driven plasma wake field acceleration (LWFA). The advantage of accelerators based on plasmas, is that they can sustain electric fields up to tens of GV/m, without electric short-circuiting, and have a potential to be a smaller and cheaper than the conventional accelerators. An electrostatic wave in plasma, co-propagating with a charged-particle bunch/beam, can keep the bunch in a high-field region over a path of a meter or more, thus transferring substantial amounts of energy to the particles in a compact space. However, the precision engineering is required to accelerate particles efficiently and uniformly and this has been a challenge.

Recently authors of Ref.[5] have taken a leap forward in PWFA. In their plasma wake field accelerator, the plasma wave is created by a 20-GeV electron bunch from SLAC's linac. A second bunch of equally energetic electrons follows close behind. With SLAC's purpose-built Facility for Advanced Accelerator Experimental Tests (FACET) [2], authors could place the trailing bunch at just the right spot in the plasma wave to increase the bunch energy by 1.6 GeV over just 30 cm of plasma. In Ref.[5] 3D particle-in-cell (PIC) simulations with resolution of  $512^3$  spatial grids of a plasma wake field interaction with beam were also carried out. They established that the drive bunch clears away the plasma electrons, leaving a region of strong but inhomogeneous electric field in its wake. If the trailing bunch is large enough and positioned in the right spot, it can flatten the electric field so that the trailing bunch is uniformly accelerated [5]. Thus, PWFA is an attractive concept to achieve the acceleration of about 74 pC of charge contained in the core of the trailing bunch in an accelerating gradient of about 4.4 GV/m. These core particles gain about 1.6 GeV of energy per particle, with a final energy spread as low as 0.7 % (2.0 % on average), and an energy-transfer efficiency from the wake to the bunch that can exceed 30 % (17.7 % on average). This acceleration of a distinct bunch of electrons containing a substantial charge and having a small energy spread with both high accelerating gradient and high energy-transfer efficiency represents a milestone in the development of PWFA into a compact and affordable accelerator technology. Despite these ground breaking advances there is a room for improvements: (i) An energy gain by the core electron bunch of about 10% can potentially be improved. (ii) From the 800 pC that started out in the trailing bunch, only 74 pC remained in the accelerated core. Better preservation of the beam is a priority for future work. (iii) Previous numerical simulations of PWFA have predicted the hosing instability to be disrupting the efficient acceleration. This has not been observed in the experiments [2, 5, 6]. Further work is needed to settle this issue.

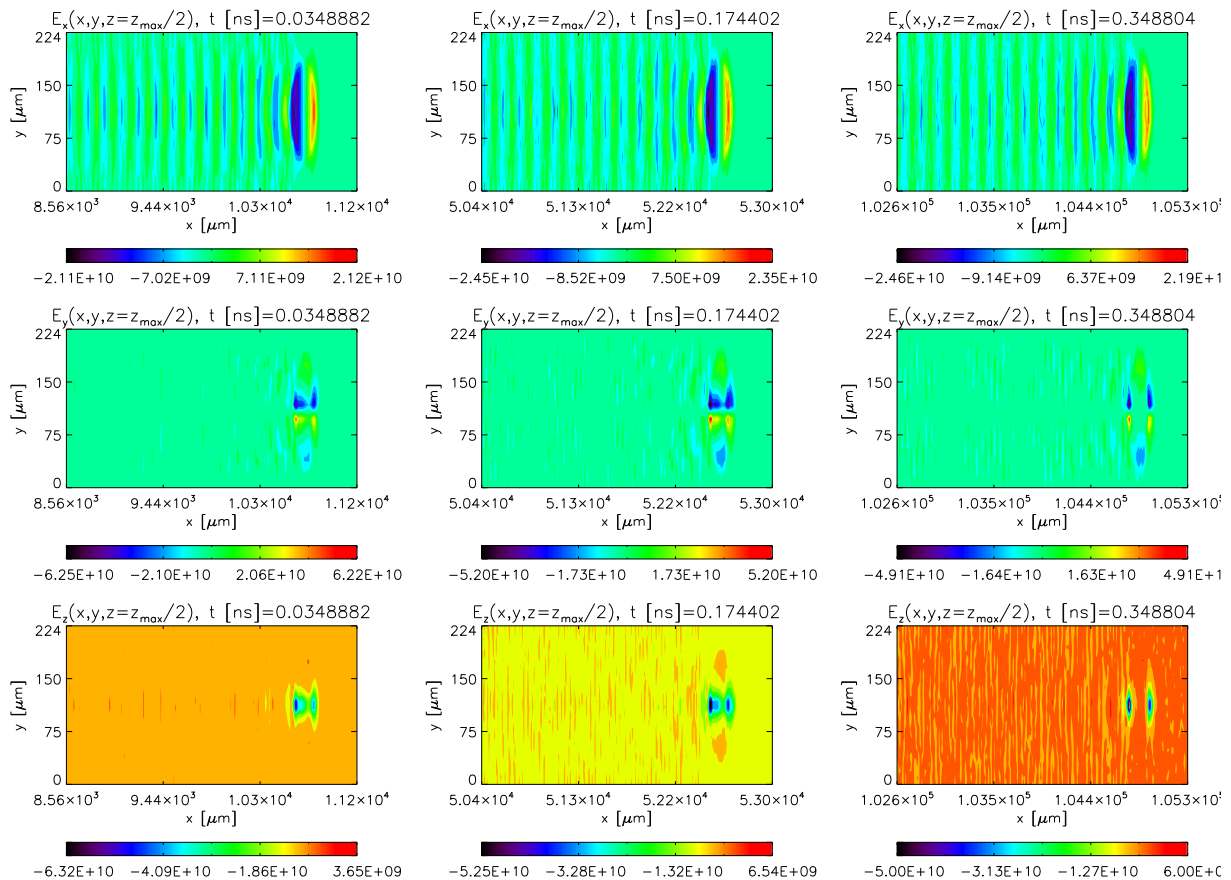


FIG. 1: Contour plots of electric field  $x$ - (top row),  $y$ - (middle row) and  $z$ - (bottom row) components in  $(x,y)$  plane (cut through  $z = z_{max}/2$ ) at different time instants corresponding to 1/10th, half and the final simulations times. The fields on color bars are quoted in  $V/m$  and time at the top of each panel is in nano-seconds. The data is for uniform density run.

Recently an interesting opportunity has been explored by Ref.[8]. In this work a beam of accelerated electrons was injected into a magnetized, Maxwellian, homogeneous, and inhomogeneous background plasma. It was established that in the case of increasing density along the path of an electron beam wave-particle resonant interaction of Langmuir waves (the same type of wave as in PWFA) with the beam electrons leads to an efficient particle acceleration. This is because Langmuir waves drift to smaller wave-numbers,  $k$ , allowing them to increase their phase speed,  $V_{ph} = \omega/k$ , and, therefore, being subject to absorption by faster electrons. This is a novel aspect and has not been yet explored in the PWFA context. Therefore the main motivation for this study is to explore the effect of longitudinal density gradient on electron plasma wake field acceleration.

Section II presents the model and results. Section III summaries the main findings.

## II. THE MODEL AND RESULTS

The simulation is carried out using EPOCH, a fully electromagnetic (EM), relativistic PIC code [1]. EPOCH is freely available for download from <https://cfsa-pmw.warwick.ac.uk>. In total seven numerical runs were carried out. Three runs with uniform, increasing (positive) and negative (decreasing) density gradients in three and two spatial dimensions (3D and 2D), and one run with uniform density in one spatial dimension (1D). Only 3D results are presented here. See supplemental material at <http://ph.qmul.ac.uk/~tsiklauri/pwfa1> for the seven input parameter files used in the simulation. The simulation parameters are similar to SLAC's FACET experiment [2] and to Ref.[5]. In uniform density runs plasma number density is set to  $n_e = n_i = n_0 = 5 \times 10^{22} \text{ m}^{-3}$ . As described in Ref.[7], plasma source in such experiments as FACET is produced by photo-ionization of Lithium vapor contained in heat-pipe oven. Here similar parameters are used: Lithium plasma temperature of  $T = 2.5 \times 10^4 \text{ K}$  and mass

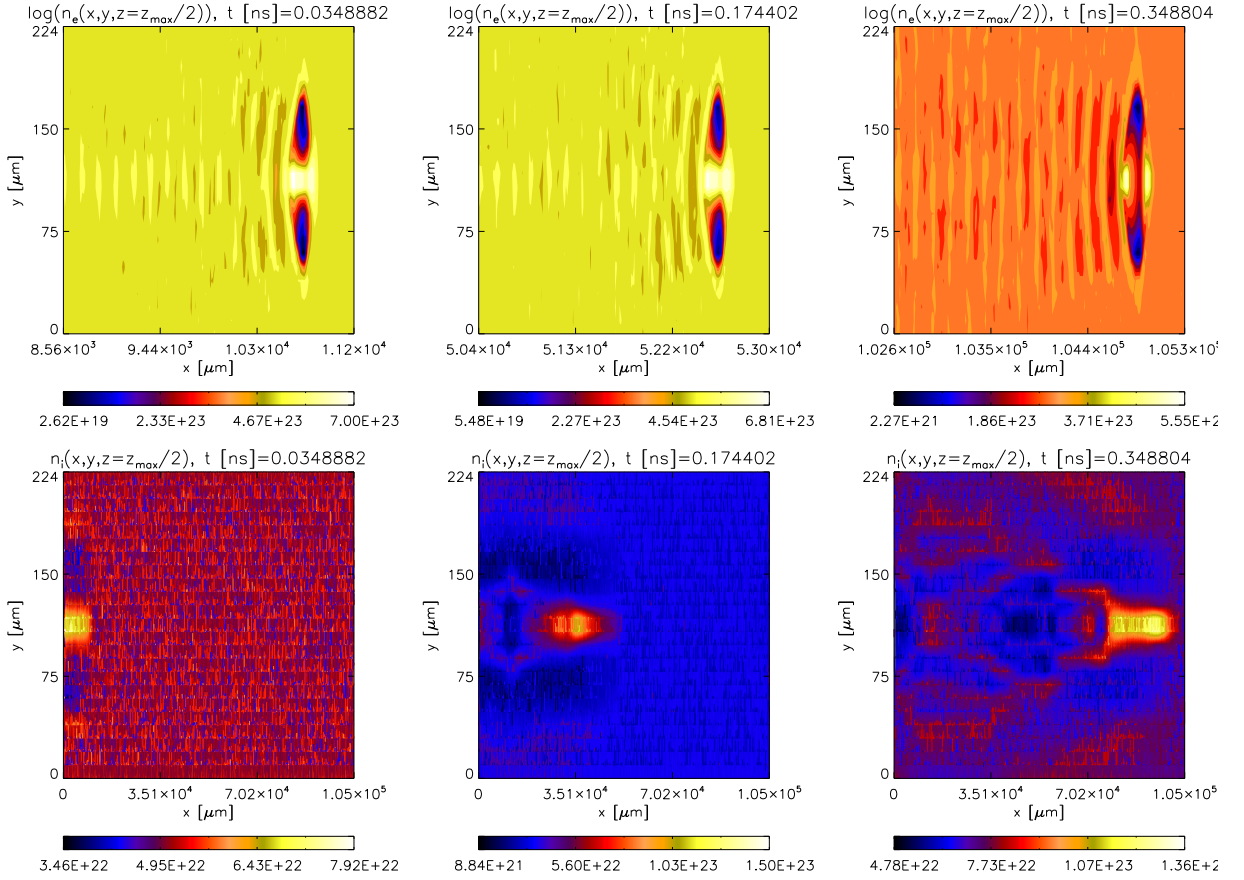


FIG. 2: Contour plots of logarithm of electron (top row) and ion (bottom row) in  $(x,y)$  plane (cut through  $z = z_{max}/2$ ) at different time instants corresponding to 1/10th, half and the final simulations times. The number densities on color bars are quoted in  $m^{-3}$  and time at the top of each panel is in nano-seconds. The data is for uniform density run.

ratio of  $m_i/m_e = 12853.1$ . Both electron bunch temperatures are also set to  $T_b = 2.5 \times 10^4$  K, producing a very narrow energy/velocity distribution spread (see the two bottom panels in Fig.3). The simulation domain is split into  $n_x \times n_y \times n_z = 7992 \times 24 \times 24$  grid cells in  $x$ -,  $y$ - and  $z$ -directions, respectively. The actual simulated domain size is within following bounds  $0 \leq x_{max} \leq 10.529748$  cm and  $0 \leq y_{max}, z_{max} \leq 234.229$   $\mu m$ . This implies the unit grid size in  $x$ -direction is  $270\lambda_D$ , while in  $y$ - and  $z$ -directions grid size is  $200\lambda_D$ . Here  $\lambda_D = v_{th,e}/\omega_{pe} = 0.048798$   $\mu m$  is the Debye length, with  $v_{th,e}/c = \sqrt{k_B T/m_e}/c = 0.00205332$  being electron thermal speed and  $\omega_{pe} = 1.2614673 \times 10^{13}$  Hz rad is the plasma frequency. It maybe counter-intuitive that simulations with under-resolved Debye length are valid. The validity is two-fold: (i) the typical total energy error in our simulations (see e.g. Fig.4) is 0.00065; (ii) the experimentally validated simulation results of Ref.[5] use  $512^3$  grids, which means their grid sizes in  $y$ - and  $z$ -directions are under-resolved by a factor of  $4918/512 = 9.6$  (this is because  $4918\lambda_D$  fit into their  $y$ - and  $z$ -direction domain sizes of  $240$   $\mu m$ ). Thus it is acceptable to under-resolve Debye length in such simulations as the electron beams are in blow out regime. This is understandable, because in plasma PIC simulation unscreened electric fields, within the under-resolved Debye sphere, lead to onset of numerical instabilities that result in what is known as "numerical heating". The latter manifests itself through the total energy increase. On contrary, because finite differencing always leads to a numerical diffusion, the total energy must decrease in time. When it increases in time this means that numerical instability is triggered. However, if the total energy error (see e.g. Fig.4) is 0.00065 (i.e. 0.065 percent) such simulations are acceptable. The possible reason why under-resolving of Debye length by factor of 200 in the transverse direction is acceptable, is because resolving  $\lambda_D$  is usually needed to correctly treat collective plasma effects such as plasma oscillation. For the plasma wake field acceleration the relevant spatial scale is electron inertial length  $c/\omega_{pe}$ . For the parameters considered  $c/\omega_{pe} = 23.765183$   $\mu m$  which means that this spatial scale is resolved with  $23.765/(200 \times 0.0488) = 2.4$  grid points (recall that  $\lambda_D = 0.048798$   $\mu m$ ). This is not ideal, but since the energy error is small the results are valid, as typically acceptable level of error is  $\approx 0.1 - 1\%$ .

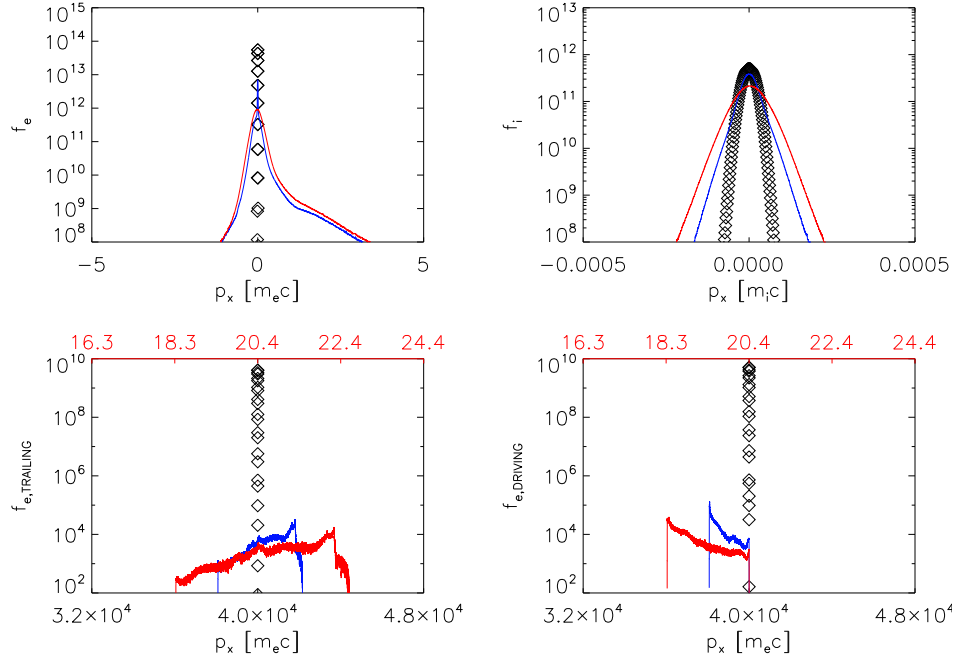


FIG. 3: Background electron (top-left), ion (top-right), trailing (bottom-left) and driving (bottom-right) electron bunch distribution functions at different times: open diamonds correspond to  $t = 0$ , while blue and red curves to the half and the final simulation times, respectively. x-axis are momenta quoted in the units of relevant species mass times speed of light i.e.  $[m_e c]$  or  $[m_i c]$  as shown on each panel. In the two bottom panels, at the top the energy is quoted in GeV with red numbers, to aid eye visualizing of trailing bunch acceleration and driving bunch deceleration processes. The data is for uniform density run.

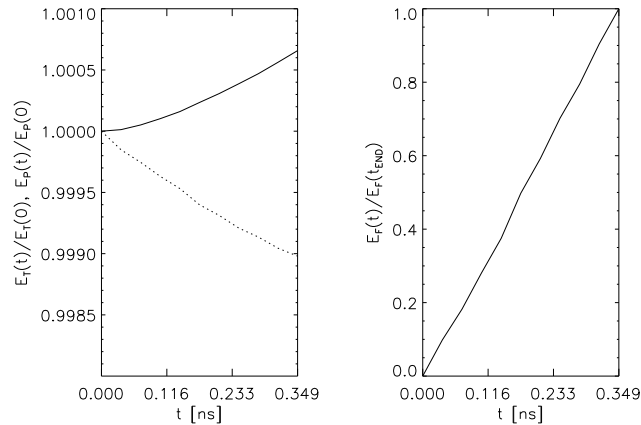


FIG. 4: Left panel's solid and dashed curves are the total (particles plus EM fields) and particle energies, normalized on initial values, respectively. Right panel shows EM field energy normalized on its final simulation time value (because it is zero at  $t = 0$ ). The data is for uniform density run.

In the positive density gradient runs, presented in figures 5, 6, 7 and 8, plasma (both background electrons and ions) number densities vary with distance  $x$ , in meters, as:

$$n_{PG}(x) = n_0 \left( 1.0 + \frac{9.0x}{x_{max}} \right) \left[ \tanh \left( \frac{x}{0.005x_{max}} \right) + \tanh \left( -\frac{x - x_{max}}{0.005x_{max}} \right) - 1.0 \right]. \quad (1)$$

This implies that the density rises from zero to  $n_0$  over a length of 1 mm, then keeps linearly rising to  $10n_0$  and in the final 1 mm of the domain it falls to zero again. In equations 1-4 the distances are quoted in meters.

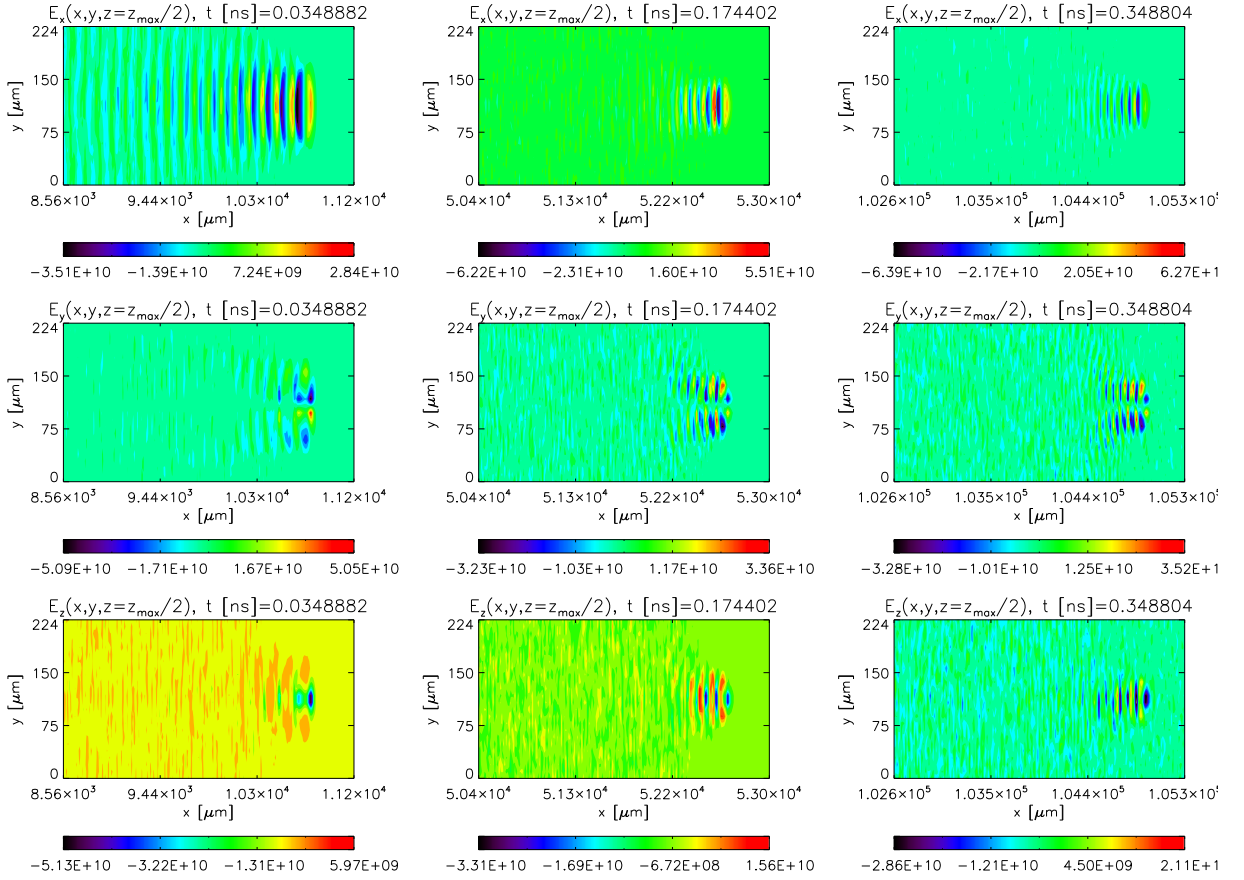


FIG. 5: As in Fig.1 but for the case of positive density gradient, according to equation 1.

In the negative density gradient runs, presented in figures 9, 10, 11 and 12, plasma number densities vary with distance  $x$  as:

$$n_{NG}(x) = n_0 \left( 1.0 - \frac{0.9x}{x_{max}} \right) \left[ \tanh \left( \frac{x}{0.005x_{max}} \right) + \tanh \left( -\frac{x - x_{max}}{0.005x_{max}} \right) - 1.0 \right]. \quad (2)$$

This implies that the density rises from zero to  $n_0$  over a length of 1 mm, then keeps linearly decreasing to  $0.1n_0$  and in the final 1 mm of the domain it falls to zero again. Such background density profiles (equations 1 and 2) allow to use periodic boundary conditions, which are used in all numerical simulations presented.

The trailing and driving electron *bunches* have the number densities as follows:

$$n_T(x) = n_0 \exp \left[ -\frac{(x - 10.0c/\omega_{pe})^2}{2.0(2.0c/\omega_{pe})^2} \right] \exp \left[ -\frac{(y - y_{max}/2.0)^2}{2.0(c/\omega_{pe})^2} \right] \exp \left[ -\frac{(z - z_{max}/2.0)^2}{2.0(c/\omega_{pe})^2} \right], \quad (3)$$

$$n_D(x) = 2.5n_0 \exp \left[ -\frac{(x - 15.7c/\omega_{pe})^2}{2.0(c/\omega_{pe})^2} \right] \exp \left[ -\frac{(y - y_{max}/2.0)^2}{2.0(c/\omega_{pe})^2} \right] \exp \left[ -\frac{(z - z_{max}/2.0)^2}{2.0(c/\omega_{pe})^2} \right]. \quad (4)$$

These expressions imply that trailing bunch is centered on  $10.0c/\omega_{pe} = 237.65183 \mu\text{m}$ , has x-length of  $\sigma_x = 2.0c/\omega_{pe} = 47.530365 \mu\text{m}$ , while driving bunch is 2.5 denser than both the background and trailing bunch, is centered on  $15.7c/\omega_{pe} = 373.11337 \mu\text{m}$  and has x-length of  $\sigma_x = c/\omega_{pe} = 23.765183 \mu\text{m}$ . The distance between the trailing and driving bunches is  $5.7c/\omega_{pe} = 135.46154 \mu\text{m}$ . This is the crucial parameter because the typical measured and simulated longitudinal scale of the plasma wake field for the density of  $n_0 = 5 \times 10^{22} \text{ m}^{-3}$  is about  $200 \mu\text{m}$  [5]. Thus the trailing bunch should lag behind the driving bunch by lesser than this length. Our bunch separation of  $\approx 135 \mu\text{m}$  sits comfortably within this range. Both electron bunches have y- and z-lengths of  $\sigma_{y,z} = c/\omega_{pe} = 23.765183 \mu\text{m}$  and are centered on  $y_{max}/2 = z_{max}/2 = 117.11432 \mu\text{m}$ .

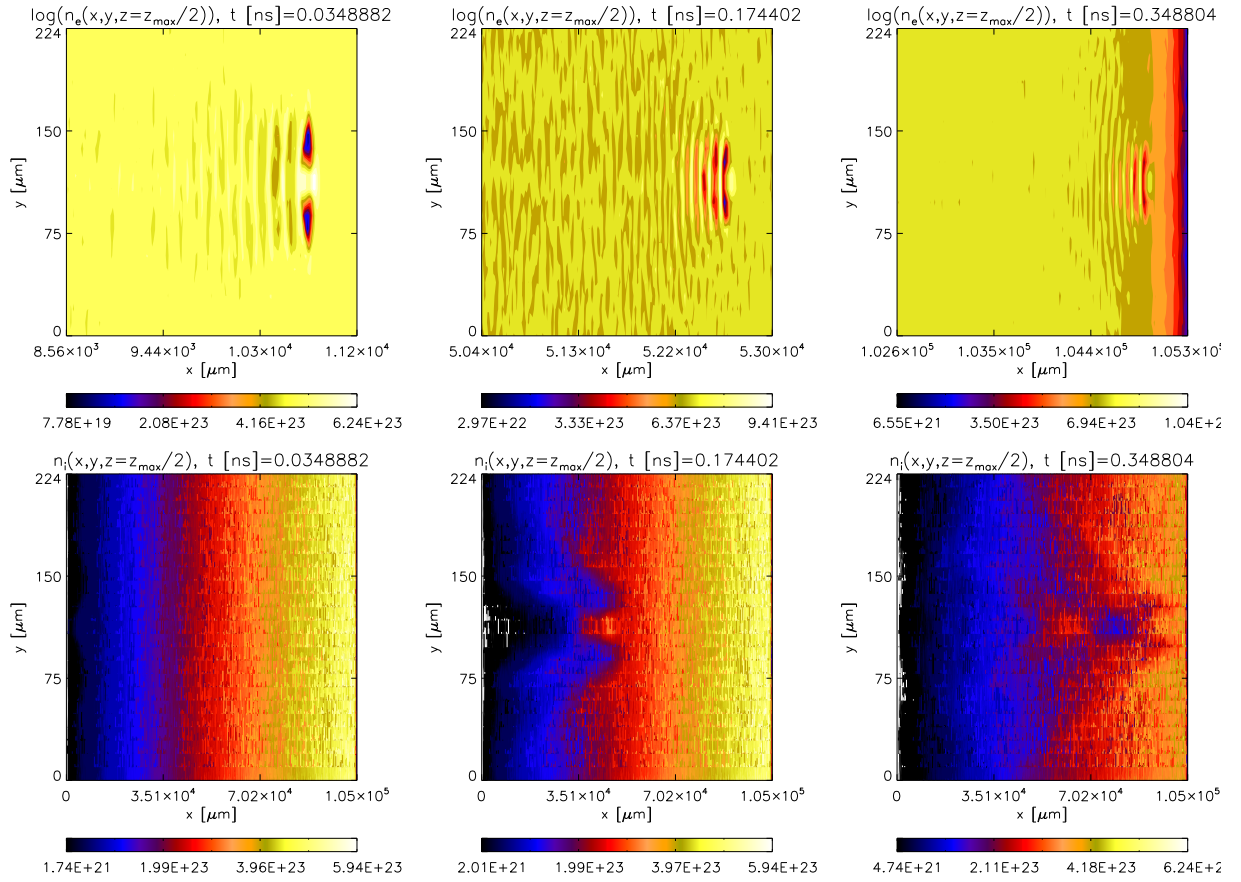


FIG. 6: As in Fig.2 but for the case of positive density gradient, according to equation 1.

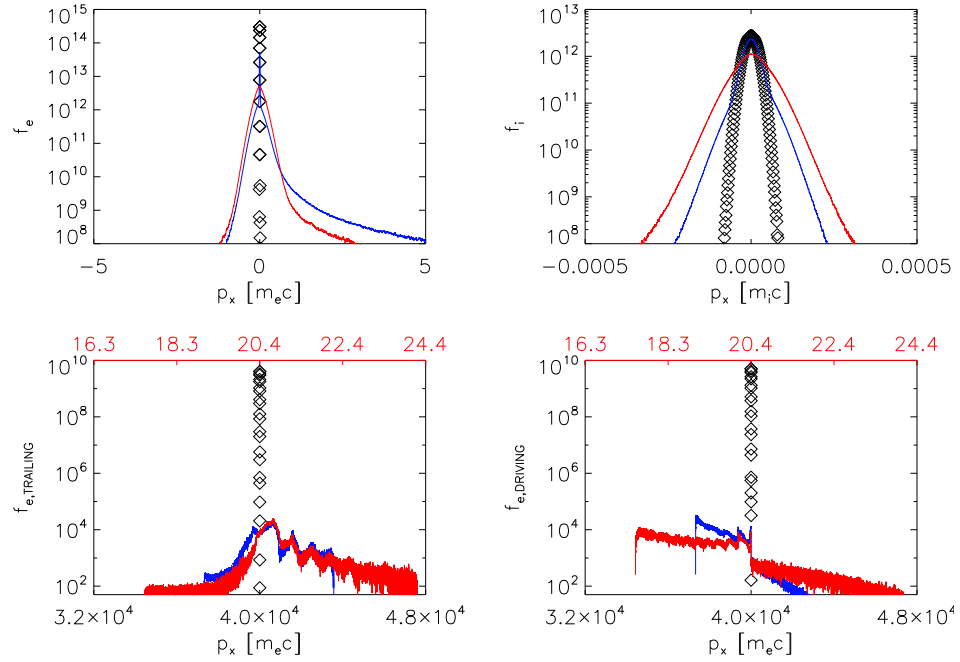


FIG. 7: As in Fig.3 but for the case of positive density gradient, according to equation 1.

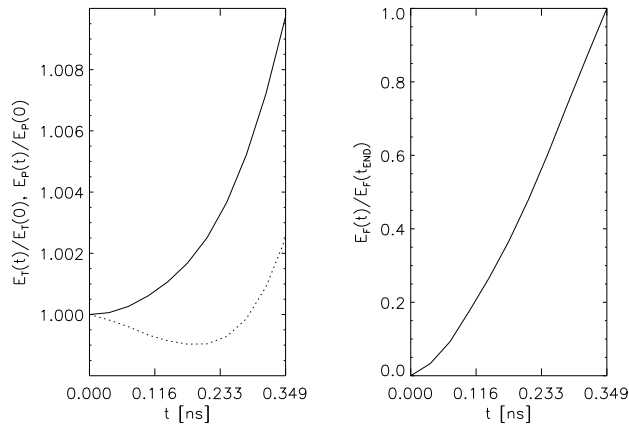


FIG. 8: As in Fig.4 but for the case of positive density gradient, according to equation 1.

Both electron bunch initial momenta are set to  $p_x = p_0 = 1.087587 \times 10^{-17} \text{ kg m s}^{-1}$  (note that  $p_x/(m_e c) = 39825.1$ ), which corresponds to an initial energy of  $E_0 = 20.35 \text{ GeV}$ . There are four plasma species present in all numerical simulations. In the 3D runs there are 73,654,272 particles for each of the four species i.e. roughly  $3 \times 10^8$  particles in total. In the 2D runs there are 34,525,440 particles for each of the four species, while in 1D each species have 1,438,560 particles. The three dimensional runs take about 27 hours on 192 computing cores, using Intel Xeon E5-2650 16-core 2.6GHz CPUs with 64 Gb of random access memory (RAM). These use  $n_x \times n_y \times n_z = 12 \times 4 \times 4$  domain decomposition for optimal code performance, particularly alleviating the particle dynamical load balancing overheads. The bottle neck for this type of simulations is the amount of RAM on each of the 16-core nodes. With twelve nodes the total of  $12 \times 64 = 768 \text{ Gb}$  of RAM was available. Background electrons and ions are distributed evenly over 192 cores, but driving and trailing bunches are very localized and move with nearly at the speed of light. This puts tight limitation on number of particles that can be used to resolve bunch electrons because both bunches must fit computationally on the 64 Gb RAM compute nodes they fly through.

Ref.[5] used QuickPIC [3] fully relativistic, 3D, particle-in-cell model bespoke for simulating plasma and laser wake field acceleration. QuickPIC is based on the quasi-static approximation, which reduces a fully 3D, EM field solve and particle push into two spatial dimensions. This is achieved by calculating the plasma wake based on the assumption of drive beam and/or laser not evolving during the time it takes for it to pass a plasma particle. The complete EM fields of the plasma wake and its associated index of refraction are then used to evolve the drive beam and/or laser using large time steps. Ref.[3] suggests that the algorithm reduces the computation time by 2 to 3 orders of magnitude without loss of accuracy. In our numerical work the EPOCH code [1] is used which is free from simplifying assumptions of QuickPIC, i.e. it is an explicit, fully electromagnetic, relativistic PIC code. Thus, it is interesting to compare the findings of both approaches.

### A. Uniform density case

Fig.1 top row shows contour plots of electric field  $E_x$  component at three times. It can be seen that the yellow half-ellipse, representing positive  $E_x \approx 2.2 \times 10^{10} \text{ V/m}$  plasma wake remains nearly constant in shape and its amplitude and travelled correct distances of  $0.0349 \times 10^{-9} \times c = 10463 \mu\text{m}$ ,  $0.1744 \times 10^{-9} \times c = 52283 \mu\text{m}$  and  $0.3488 \times 10^{-9} \times c = 104567 \mu\text{m}$  within the corresponding times. Also it can be seen that negative,  $E_x \approx -2.5 \times 10^{10} \text{ V/m}$ , the dark blue half-ellipse, closely follows the yellow one. It is this region of negative  $E_x$  that accelerates the trailing bunch. Ref.[5] has not presented the transverse EM field dynamics. This is shown in the middle and lower rows of Fig.1. In Fig.1 middle row shows contour plots of electric field  $E_y$  component at three times. It can be seen that  $E_y$  has quadrupolar structure with two positive peaks on the right side and two negative dips on the left side of the drive bunch path. The amplitudes of the quadrupolar  $E_y \approx \pm 5 \times 10^{10} \text{ V/m}$  and are co-located (across x-position) with  $E_x$  positive and negative electrostatic wakes. Fig.1 lower row shows contour plots of electric field  $E_z$  component at three times.  $E_z$  fields show two localized dips with amplitudes of  $E_z \approx -5 \times 10^{10} \text{ V/m}$  that are also spatially co-located with  $E_x$  positive and negative electrostatic wakes. Note that in the bottom row of Fig.1 background around the electron bunches appears yellowish color instead of green that corresponds to zero level. This is because of the presence of

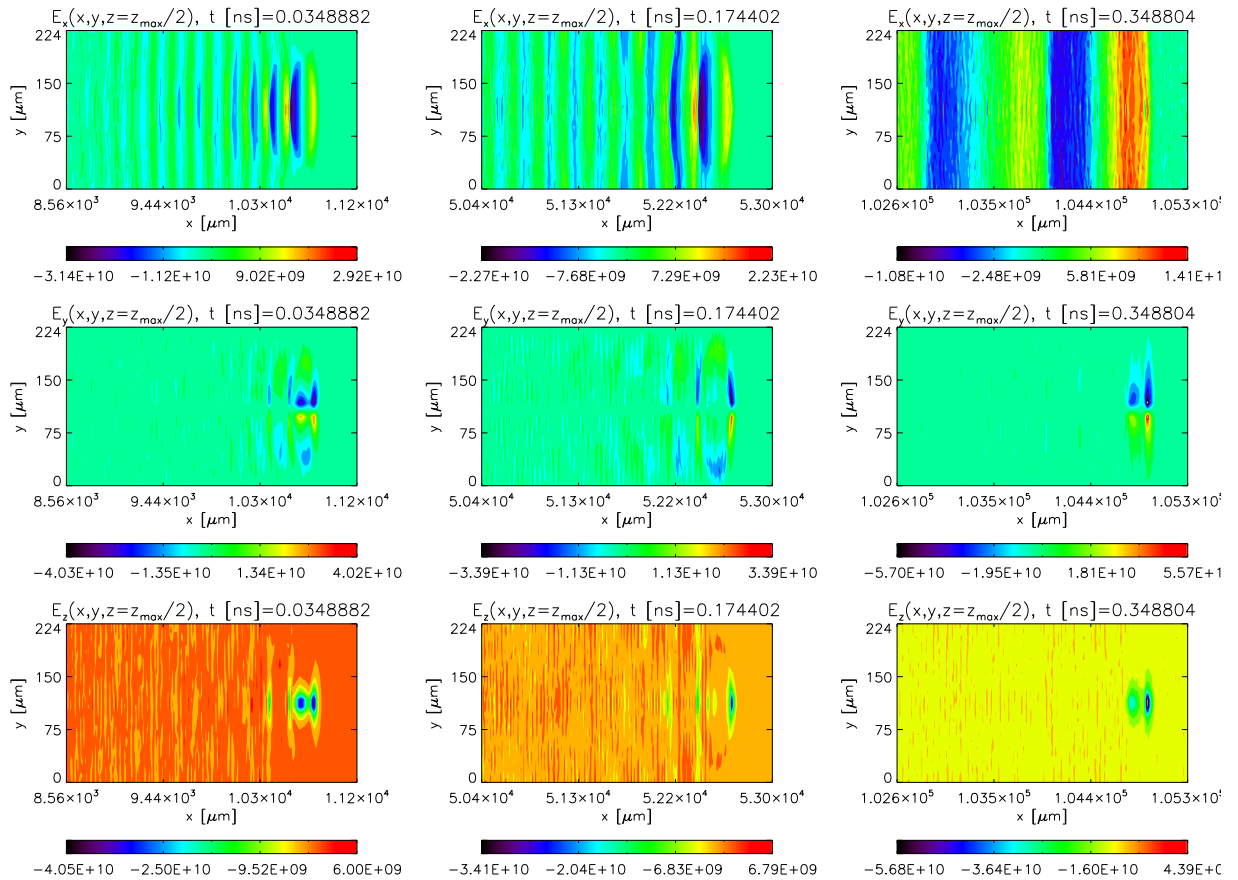


FIG. 9: As in Fig.1 but for the case of negative density gradient, according to equation 2.

noise, which in principle can be averaged out to make background green (zero), but this averaging distorts the shape of the two dips in  $E_z$  and hence the averaging was not performed.

Fig.2 shows contour plots of logarithm of electron (top row) and ion (bottom row) number densities in  $(x,y)$  plane (cut through  $z = z_{max}/2$ ) at different time instants. Here the electron number density includes contributions from background electrons, trailing and driving electron bunches (i.e. all electrons in the simulation). It can be seen that the transverse electric field of the driving bunch expels electrons creating two density cavities with about  $50 \mu\text{m}$  size in  $y$ -direction and  $130 \mu\text{m}$  size in  $x$ -direction. The latter distance is estimated as roughly  $(1/7)$ th of distance between  $x = 1.12 \mu\text{m}$  and  $x = 1.03 \mu\text{m}$  i.e.  $(1.12 - 1.03) \times 10^4 / 7 \approx 130 \mu\text{m}$ . This is consistent with the previous results of Ref.[5]. The novelty is, however, in the inclusion of mobile ions. It can be seen from bottom row panels in Fig.2 that ion density perturbation can be as large as few times the initial ion density. The ion density increase has the size of 2000 grids which is about  $26351 \mu\text{m}$ .

Fig.3 quantifies the details of background electron, ion, trailing and driving electron bunch distribution functions at different times: open diamonds correspond to  $t = 0$ , while blue and red curves to the half and the final simulation times, respectively. It can be gathered from the plot that the background electrons develop non-thermal tails in the direction of motion of the trailing and driving electron bunches (i.e. positive  $x$ -direction) with values attaining  $p_x \approx 3 - 4 m_e c$ . Ions seem to be heated, rather than developing non-thermal tails, which can be witnessed by symmetric broadening of the distribution function. Lower left panel of Fig.3 demonstrates that by end of simulation time the trailing bunch gains energy of 22.4 GeV, starting from initial 20.4 GeV, with an energy transfer efficiencies of 65 percent. The latter is quantified by calculating: (i) The trailing bunch acceleration efficiency

$$AE(t) = \frac{\int_{p_x > p_0}^{\infty} f_{e, \text{TRAILING}}(p_x, t) dp_x}{\int_{-\infty}^{\infty} f_{e, \text{TRAILING}}(p_x, t = 0) dp_x}, \quad (5)$$

where  $p_0 = 1.087587 \times 10^{-17} \text{ kg m s}^{-1}$  which corresponds to an initial energy of  $E_0 = 20.35 \text{ GeV}$ . Note that  $p_0/(m_e c) = 39825.1$ . Using IDL's `int_tabulated` built-in function that performs five-point Newton-Cotes integration

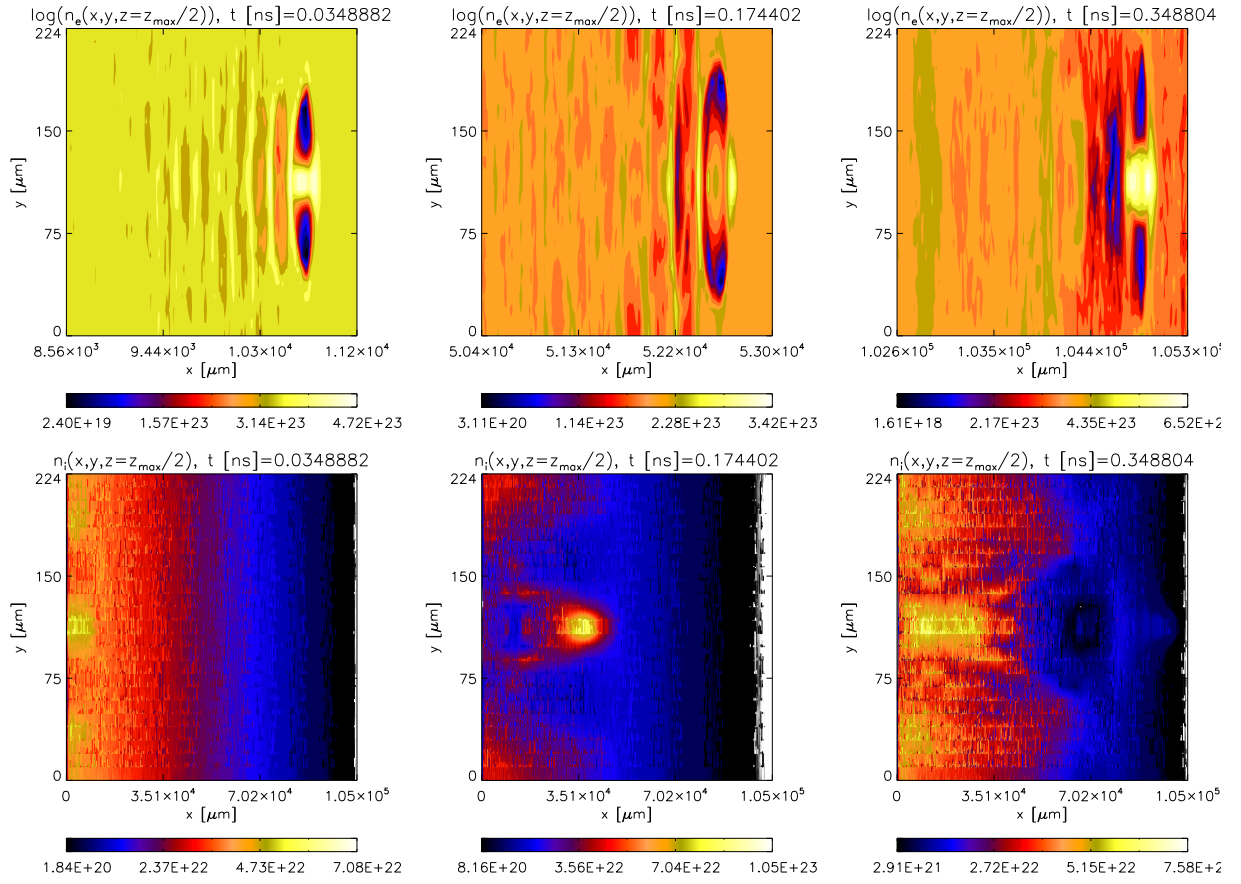


FIG. 10: As in Fig.2 but for the case of negative density gradient, according to equation 2.

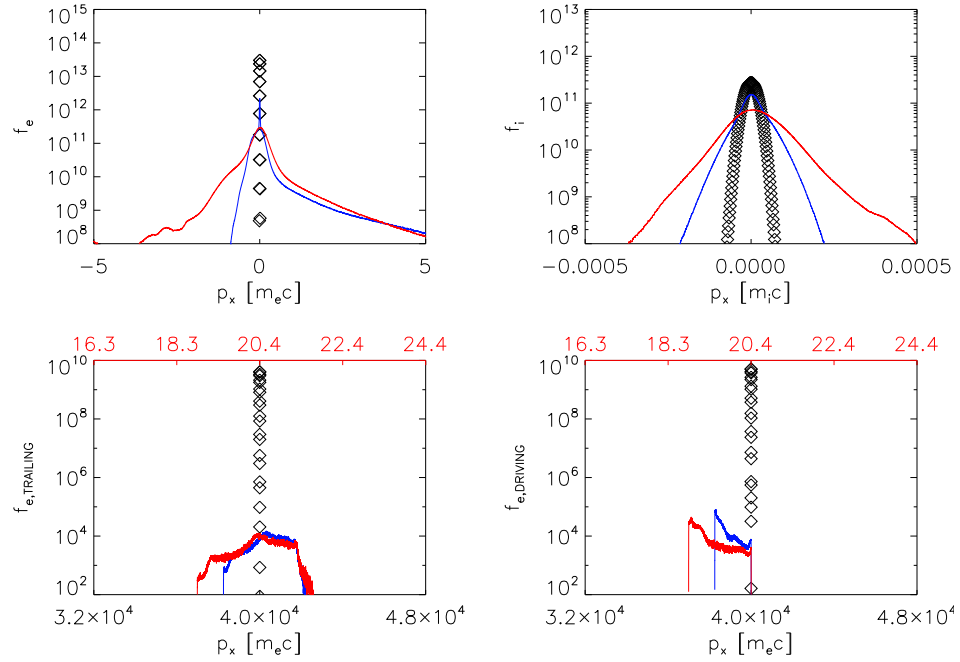


FIG. 11: As in Fig.3 but for the case of negative density gradient, according to equation 2.

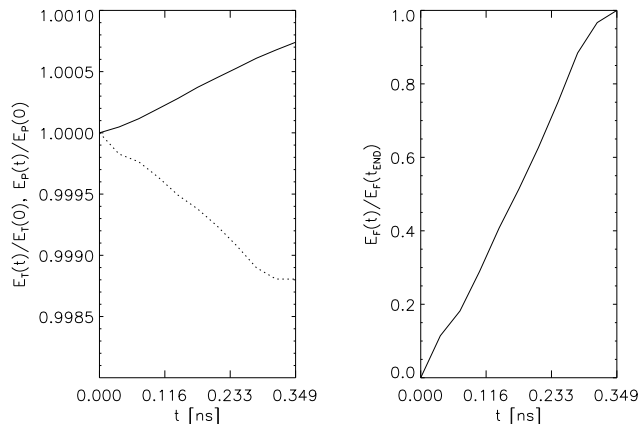


FIG. 12: As in Fig.4 but for the case of negative density gradient, according to equation 2.

with  $10^8$  grid points in the  $p_x$ , the values for data of uniform density 3D run are:  $AE(t = 0.1744 \text{ ns}) = 0.6677$ ,  $AE(t = 0.3488 \text{ ns}) = 0.6674$ . All numerical runs use  $10^8$  grid points in the  $p_x$ , thus, we are confident that indexes  $AE(t)$  and  $TE(t)$  are calculated accurately. (ii) The energy transfer efficiency from the driving bunch to trailing bunch

$$TE(t) = \frac{\int_{p_x > p_0}^{\infty} f_{e, \text{TRAILING}}(p_x, t) dp_x}{\int_{-\infty}^{p_0} f_{e, \text{DRIVING}}(p_x, t) dp_x}. \quad (6)$$

The values for data of uniform density 3D run are:  $TE(t = 0.1744 \text{ ns}) = 0.6476$ ,  $TE(t = 0.3488 \text{ ns}) = 0.6463$ . Note that the physical meaning of  $AE(t)$  is the fraction of trailing bunch electrons with momenta greater than  $p_0$  (or with energies greater than  $E_0 = 20.35 \text{ GeV}$ ) of the total number of trailing bunch electrons at  $t = 0$ . The physical meaning of  $TE(t)$  is the fraction of trailing bunch electrons with momenta greater than  $p_0$  (or with energies greater than  $E_0 = 20.35 \text{ GeV}$ ) of the number of driving bunch electrons with momenta less than  $p_0$  at time  $t$  (not at  $t = 0$  – compare the denominators of Equations 5 and 6 and note the different times  $t$  used). Because the energy of accelerated trailing bunch electrons comes from the deceleration of driving bunch electrons, the both indexes  $AE(t)$  and  $TE(t)$  have similar values of 65 percent. Equations 5 and 6 contain infinite integration bounds  $\pm\infty$ . The employed discretized version has instead bounds of  $p_{x, \text{MAX}, \text{MIN}} = \pm 1.4 \times 10^{-17} \text{ kg m s}^{-1}$ . The range was split into 100 million points. Thus calculation of  $AE(t)$  and  $TE(t)$  indexes is accurate. Lower right panel of Fig.3 demonstrates that by the end of simulation time starting from initial 20.4 GeV, the driving bunch loses energy to about 18.3 GeV.

Left panel of Fig.4 shows the behavior of the total (particles plus EM fields) and particle energies, normalized to initial values, respectively. It can be seen that the total energy increases due to numerical heating, but stays within a tolerable value of 0.065 percent. The particle energy decreases by 0.1 percent. The right panel shows EM field energy normalized to its final simulation time value. It can be seen that it steadily increases as the plasma wake is generated.

## B. Positive density gradient case

Next, the effect of positive density gradient on PWFA is investigated. Fig.5 is similar to Fig.1, but for the case of positive density gradient, according to equation 1. It can be gathered from top row of Fig.5 that electrostatic plasma wake becomes spatially localized and, compared to the homogeneous density 3D case,  $E_x$  now attains three times larger values of  $\pm 6.5 \times 10^{10} \text{ V/m}$ . This can be explained by the fact that plasma wake size is prescribed by the electron inertial length,  $c/\omega_{pe}$ . Hence, because of the scaling law  $\omega_{pe} \propto \sqrt{n_e}$ , the progressively increasing density, into which driving bunch plows through, creates more localized and stronger wake. Also more oscillations (peaks and troughs) in the wake can be seen. This is because the plasma wake is oscillating spatially at  $\omega_{pe}$ , which is increasing with the increase of number density.

Fig.6 is similar to Fig.2 but for the case of positive density gradient numerical simulation run, which uses density gradient prescribed by equation 1. It can be seen that, in this case, electron density cavities are more compact too, commensurate with a more compact electrostatic wake. The blue strip in the rightmost panel of top row in Fig.6 is due to background density falling off to zero, as prescribed by the initial conditions. In the ion density (bottom row)

because x-axis spans entire domain, background density ten-fold increase is clearly seen. Ion density perturbation is less profound because it is now on top of the background density ten-fold increase (due to the background density gradient).

Fig.7 is as in Fig.3 but for the case of positive density gradient, according to equation 1. The top row shows that background electron positive momenta tail is now *intermittently* more energetic, compared to the uniform density 3D case and also ion heating is intermittently more stronger. Bottom left panel shows that trailing bunch energies reach as high as 24.4 GeV. The acceleration and energy transfer efficiencies in this case are calculated as follows:  $AE(t = 0.1744 \text{ ns}) = 0.6100$ ,  $AE(t = 0.3488 \text{ ns}) = 0.7326$  and  $TE(t = 0.1744 \text{ ns}) = 0.6052$ ,  $TE(t = 0.3488 \text{ ns}) = 0.7545$ , indicating about 75 percent acceleration and energy transfer efficiency by the end simulation time. The bottom right panel shows that driving bunch partly decelerates and partly accelerates, i.e. red curve now spreads beyond  $E_0$ . This can be attributed to re-acceleration of driving bunch due to the positive density gradient. Ref.[8] established that in the case of increasing density along the path of an electron beam wave-particle resonant interaction of Langmuir waves with the beam electrons leads to an efficient particle acceleration. This is because Langmuir waves drift to smaller wavenumbers  $k$ , allowing them to increase their phase speed,  $V_{ph} = \omega/k$ , and, thus, being absorbed by faster electrons. Because the simulations are in the blow out regime, driving beam number density is 2.5 times denser than background electron density, Langmuir waves will grow via bump-on-tail instability on the time scale of  $\approx 1/2.5 = 0.4\omega_{pe}^{-1}$ . The final simulation time of 0.3488 ns corresponds to  $4400\omega_{pe}^{-1}$ . Thus there will be a plenty of time for the above described effect of re-acceleration of driving bunch due to the positive density gradient [8] to take place.

Fig.8 is as in Fig.4 but for the case of positive density gradient, according to equation 1. It can be seen that now total energy error is just under 1 percent. This is larger than in the uniform density 3D case, but possibly still tolerable.

### C. Negative density gradient case

Next, the effect of negative density gradient on PWFA is investigated. Fig.9 is similar to Fig.1, but for the case of negative density gradient, according to equation 2. It can be seen in top row of Fig.9 that electrostatic plasma wake becomes spatially wider spread, compared to the homogeneous density 3D case, with larger distances between the peaks and troughs in x-direction. In the transverse y-direction size of the wake grows too, such that by the end of simulation the wake is larger than  $y_{max} = 234.229 \mu\text{m}$  (note that data up to 23-rd grid point is plotted, cutting off plot at  $224 \mu\text{m}$ ).  $E_x$  now attains two-and-a-half times smaller value of  $-1.1 \times 10^{10} \text{ V/m}$ . Again, this can be explained by the fact that plasma wake size is prescribed by the electron inertial length,  $c/\omega_{pe} \propto 1/\sqrt{n_e}$ . Thus, progressively decreasing density creates less localized, wider-spread and thus weaker plasma wake. Also lesser number of oscillations (peaks and troughs) in the wake is seen. This is because the plasma wake is oscillating spatially at  $\omega_{pe}$ , which is decreasing with the decrease of number density. Surprisingly, transverse EM fields (middle and bottom rows in Fig.9) are similar in their structure to that of homogeneous density case (middle and bottom rows in Fig.1). On the contrary, in positive density gradient case (middle and bottom rows in Fig.5) more localized  $E_y$  and  $E_z$  is seen. Thus, it is concluded that negative gradient affects only electrostatic,  $E_x$  component and not  $E_y$  or  $E_z$ .

Fig.10 is as in Fig.2 but for the case of negative density gradient, according to equation 2. It can be seen that, in this case, electron density cavities are larger in size, commensurate with a more wider-spread electrostatic wake. In the ion density (bottom row) because x-axis spans entire domain, background density ten-fold decrease is clearly seen. This decrease is prescribed by equation 2. Ion density perturbation is of the same order as the background density.

Fig.11 is as in Fig.3 but for the case of negative density gradient, according to equation 2. The top row shows that background electron positive momenta tail is now more energetic compared to the uniform density 3D case and also ion heating is more stronger. The bottom left panel shows that trailing bunch energies reach only 21.4 GeV. The acceleration and energy transfer efficiencies in this case are calculated as follows:  $AE(t = 0.1744 \text{ ns}) = 0.6187$ ,  $AE(t = 0.3488 \text{ ns}) = 0.4617$  and  $TE(t = 0.1744 \text{ ns}) = 0.6004$ ,  $TE(t = 0.3488 \text{ ns}) = 0.4465$ , indicating 45 percent acceleration and energy transfer efficiency by the end simulation time. The bottom right panel shows that driving bunch only decelerates i.e. blue and red curves shifts to the left of  $E_0$ .

Fig.12 is as in Fig.4 but for the case of negative density gradient, according to equation 2. It can be seen that now total energy error is 0.065 percent, which is similar to the uniform density 3D case.

## III. CONCLUSIONS

3D, 2D and 1D, particle-in-cell, fully electromagnetic simulations of electron plasma wake field acceleration in the blow out regime have been carried out. For brevity only 3D results are presented here. Our aim was to extend earlier results of Ref.[5] by (i) studying the effect of longitudinal density gradient in the light of the results of Ref.[8];

(ii) avoiding use of co-moving simulation box because the density gradient cases require considering a long domain that fits the entire gradient; (iii) inclusion of ion motion; and (iv) studying fully electromagnetic plasma wake fields without quasi-static approximation of QuickPIC [3]. It has been shown that injecting driving and trailing electron bunches into a positive density gradient of ten-fold increasing density over 10 cm long plasma, results in spatially more compact and three times larger electric fields ( $-6.4 \times 10^{10}$  V/m), leading to acceleration of the trailing bunch up to 24.4 GeV (starting from initial 20.4 GeV), with an energy transfer efficiencies from leading to trailing bunch of 75 percent compared to the uniform density case. In the latter case  $-2.5 \times 10^{10}$  V/m wave is created leading to acceleration of the trailing bunch up to 22.4 GeV, with an energy transfer efficiencies of 65 percent. It has been shown that injecting the electron bunches into a negative density gradient of ten-fold decreasing density over 10 cm plasma, yields spatially more spread wake and two-and-half smaller electric fields ( $-1.0 \times 10^{10}$  V/m), leading to a weaker acceleration of the trailing bunch up to 21.4 GeV (starting from initial 20.4 GeV), with an energy transfer efficiencies from leading to trailing bunch of 45 percent. It was also shown (not included here) that 2D simulation results are substantially different from the 3D ones, showing only 10 percent efficiency of trailing bunch acceleration, while in 1D case understandably no acceleration is seen. This is because in 1D no transverse electric field can be sustained (because transverse directions are ignorable) and thus the driving bunch cannot expel electrons to create density cavities. The ion motions have been also included into consideration, showing that in the plasma wake ion number density can increase over few times the background value. Finally, it has been also shown that transverse electromagnetic fields in plasma wake are of the same order as the longitudinal (electrostatic) ones.

In terms of an experimental implementation of the proposed PWFA experiments with the longitudinal density gradient, it is to be remarked that: (i) The positive density gradient maybe created by driving a hollow piston in the photo-ionized Lithium vapor plasma contained in heat-pipe oven [7], as in FACET [2]. The ten-fold compression of the plasma density may be created by the piston moving in the same direction as the driving and trailing electron bunches that would fly through a hole in the piston. (ii) The negative density gradient, e.g. a ten-fold rarefaction, maybe created by pulling the hollow piston the opposite direction to the bunch's motion through a hole in the piston.

**Competing interests statement.** Author has no competing interests.

**Funding.** Author was financially supported by Leverhulme Trust Research Project Grant RPG-311.

**Acknowledgments.** Author would like to thank two anonymous referees for careful reading of the manuscript and useful suggestions. This research utilized Queen Mary University of London's (QMUL) MidPlus computational facilities, supported by QMUL Research-IT and funded by UK EPSRC grant EP/K000128/1. EPOCH code development work was in part funded by the UK EPSRC grants EP/G054950/1, EP/G056803/1, EP/G055165/1 and EP/M022463/1 to which Author has no connection.

- 
- [1] T. D. Arber, K. Bennett, C. S. Brady, A. Lawrence-Douglas, M. G. Ramsay, N. J. Sircombe, P. Gillies, R. G. Evans, H. Schmitz, A. R. Bell and C. P. Ridgers, "Contemporary particle-in-cell approach to laser-plasma modelling," *Plasm. Phys. Contr. Fus.*, vol. 57, 113001, 2015, doi:10.1088/0741-3335/57/11/113001.
  - [2] M. J. Hogan, T. O. Raubenheimer, A. Seryi, P. Muggli, T. Katsouleas, C. Huang, W. Lu, W. An, K. A. Marsh, W. B. Mori, C. E. Clayton and C. Joshi, "Plasma wakefield acceleration experiments at FACET," *New J. Phys.*, vol. 12, 055030, 2010, doi:10.1088/1367-2630/12/5/055030.
  - [3] C. Huang, V. K. Decyk, M. Zhou, W. Lu, W. B. Mori, J. H. Cooley, T. M. Antonsen Jr, B. Feng, T. Katsouleas, J. Vieira and L. O. Silva, "QuickPIC: a highly efficient fully parallelized PIC code for plasma-based acceleration," *J. Phys. Conf. Ser.*, vol. 46, pp. 190-199, 2006, doi:10.1088/1742-6596/46/1/026.
  - [4] W.D. Kilpatrick, "Criterion for Vacuum Sparking Designed to Include Both rf and dc," *Rev. Sci. Instr.*, vol. 28, pp. 824-830, 1957, doi:10.1063/1.1715731.
  - [5] M. Litos, E. Adli, W. An, C. I. Clarke, C. E. Clayton, S. Corde, J. P. Delahaye, R. J. England, A. S. Fisher, J. Frederico, S. Gessner, S. Z. Green, M. J. Hogan, C. Joshi, W. Lu, K. A. Marsh, W. B. Mori, P. Muggli, N. Vafaei-Najafabadi, D. Walz, G. White, Z. Wu, V. Yakimenko and G. Yocky, "High-efficiency acceleration of an electron beam in a plasma wakefield accelerator," *Nature*, vol. 515, pp. 92-95, 2014, doi:10.1038/nature13882.
  - [6] J.L. Miller, "Plasma wakefield acceleration shows promise," *Phys. Today*, vol. 68 (1), pp. 11-13, 2015, doi:10.1063/PT.3.2639.
  - [7] P. Muggli, K.A. Marsh, S. Wang, C.E. Clayton, S. Lee, T.C. Katsouleas and C. Joshi, "Photo-ionized lithium source for plasma accelerator applications," *IEEE Trans. Plasm. Sci.*, vol. 27, pp. 791, (1999), doi:10.1109/27.774685.
  - [8] R. Pechhacker and D. Tsiklauri, "Three-dimensional particle-in-cell simulation of electron acceleration by Langmuir waves in an inhomogeneous plasma," *Phys. Plasmas*, vol. 21, 012903, 2014, doi:10.1063/1.4863494.